ART-TOC-ENTRY

Adsorption equilibria of methyl *tert*-butyl ether (MTBE)/toluene (TOL), and 1,2-dichloroethane (DCE)/MTBE binary mixtures in aqueous solution on ZSM-5 were measured over a wide range of concentrations.

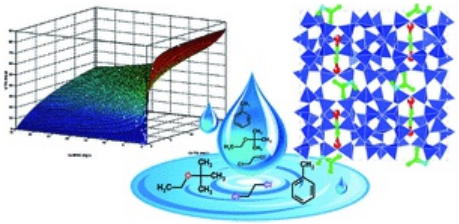

Competitive adsorption of VOCs from binary aqueous mixtures on zeolite ZSM-5†

†Electronic supplementary information (ESI) available: Pattern diffraction of ZSM-5 loaded with MTBE-TOL and DCE-MTBE mixtures. Thermogravimetry, framework and extraframework atomic coordinates, and temperature factors are provided (Tables 2–5SII)]. See DOI: 10.1039/c6ra08872d

L. Pasti,[a]

E. Rodeghero,[b]

E. Sarti,[a]

V. Bosi,[a]

A. Cavazzini,[a]

R. Bagatin,[c]

A. Martucci[b]

[a]Department of Chemistry and Pharmaceutical Sciences, University of Ferrara, Via L. Borsari 46, I-44123 Ferrara (FE), Italy.

[b]Department of Physics and Earth Sciences, University of Ferrara, Via Saragat 1, I-44123 Ferrara (FE), Italy.

[c]Research Center for Non-Conventional Energy – Istituto Eni Donegani Environmental Technologies, via Maritano, 26, San Donato Milanese (MI), I-20097, Italy.

Abstract

Adsorption equilibria of methyl *tert*-butyl ether (MTBE)/toluene (TOL), and 1,2-dichloroethane (DCE)/MTBE binary mixtures in aqueous solution on ZSM-5 were measured over a wide range of concentrations. In comparison with the single-component data, the loading of all of the three compounds was reduced in the presence of a second component in the mixture. The binary system was described by a competitive dual site Langmuir adsorption isotherm. The model was chosen on the basis of the results obtained from X-ray diffraction studies of the adsorbent material loaded with equimolar binary mixtures. Rietveld structure refinements provide information about the relative position of molecules inside the structure after TOL-MTBE and DCE-MTBE mixture adsorption. The short intermolecular distances between the adsorption sites of MTBE, DCE and TOL inside the zeolite framework clearly prevent the simultaneous occupancy of one site by more than one component, when these compounds are adsorbed from binary mixtures.

Introduction

Zeolitic materials are of great importance in many technological processes due to their unique pore topologies, the possibility to introduce active reaction sites, their relevant thermal and chemical stability, their high selectivity and rapid kinetics.[1–4] In recent years, high-silica zeolites (HSZ) have been employed as nanoscale advanced adsorbent materials to remove organic compounds from air and water, in technology aimed at controlling pollution.[5–8] In particular, HSZ are gaining a special attention for environmental applications in permeable reactive barrier (PRB) technologies, where they were recently used as adsorbents in situations of multiple and complex contamination of aquifers.[9–11] In PRB configuration, their use as extruded sorbent materials and/or membranes allowed the treatment of contaminated waters in compact systems without the use of chemical agents. Additionally, with respect to Activated Carbons (ACs) they do not suffer of fire risk, pore clogging, hygroscopicity and lack of regenerability when used for the removal of Volatile Organic Compounds (VOCs).[2,12,13] Their relevance to these areas stimulates scientists to investigate these materials and many studies have been devolved to clarify the molecular filling patterns of zeolite micropores during the adsorption of a single compound.[14–16] Indeed many works deal with the adsorption of VOCs from unary and binary mixtures in gaseous phase onto zeolites.[17–20] In the latter cases, it was reported that for a given crystalline framework, the adsorption depends on component volatility size, shape, charge, and concentration, initial molar fraction of the gas phase, as well as the Si/Al ratio of the host framework and the nature/amount of the extra-framework species.[21–23] Multicomponent adsorption from dilute aqueous solution involves solvent–adsorbate interaction and competitive adsorption of water on the adsorbent materials other than adsorbate–adsorbate and the adsorbate–adsorbent interactions; hence, the complexity of the process increases for aqueous mixture with respect to gas phase systems.[24,25] Moreover, it has been demonstrated that water significantly influences the adsorption process and the role of water on the adsorption varies with the chemical properties of the organic adsorbate.[21–23,26–28] Therefore, in the adsorption of mixtures, single sorbate interactions with a sorbent can be altered (*i.e.* competition occurs) by the presence and quantity of other sorbates and by the solvent. Knowledge of the adsorption capacity and selectivity of materials are important for the applicability of the adsorbent materials. In general, at low concentrations competitive interactions are not expected to play a significant role in the adsorption process. However, in the case of a high concentration ranges, or during the life time of the adsorbent a full understanding of the competitive interactions among adsorbates would be necessary to predict adsorbent behaviour.

As previously mentioned, zeolites have been found to efficiently adsorb many different organic compounds, however, molecular-level understanding of how the organic species dissolved in water compete for zeolite pore space remains limited. This study aims at comparing adsorption properties of a commercial hydrophobic powder zeolite ZSM-5 toward three representative water contaminants chosen as model VOCs: methyl *tert*-butyl ether (MTBE), toluene (TOL), and 1,2-dichloroethane (DCE) *via* single and binary mixtures aqueous solutions equilibria measurements. These compounds were select to represent different VOC classes (oxygenated, aromatics and chlorinated organic compounds, respectively). Moreover they have similar molar mass but different chemical physical properties. In particular, MTBE contains an ether functional group and is hydrophilic, DCE is hydrophobic and slightly polar, TOL is hydrophobic (see Table 1SI†). As adsorbent material a ZSM-5 zeolites was employed since it has been demonstrated that this zeolite is efficient in the adsorption of contaminants in low concentration range when compared to other microporous and mesoporous materials characterized by larger porosity.[21] The adducts of zeolite and binary mixture of the selected VOC are investigated by a structural approach in order to get a better understanding of the geometrical arrangement of adsorbed molecules and their chemical environment in the zeolite pores to understand the functionality of the host–guest interactions between VOCs and zeolite. The insights gained from structural refining has been employed as input of the competitive adsorption modelling. We believe that the present original approach of integrating structural information to thermodynamic equilibrium data is an excellent model system for realistically describing the adsorption process and helping in the interpretation of the adsorption mechanisms. Additionally, thanks to the different properties of the selected VOCs, adsorption studies of these species would provide insights into zeolite selectivity for VOC removal processes.

Experimental

Materials and methods

Materials

TOL (purity 99.9%), MTBE (purity 99.8%), DCE (purity 99.8%) and sodium chloride (purity 98%) were obtained from Sigma-Aldrich (Steinheim, Germany). In Table 1SI† the physical–chemical properties of the three investigated compounds are reported. The zeolite sample used in this study is a hydrophobic ZSM-5 (CBV28014, Zeolyst International) characterized by SiO_2/Al_2O_3 ~ 280, Na_2O content < 0.05% w/w, NH_4^+ content < 0.1% w/w, and surface area of 400 $m^2\ g^{-1}$.

Gas chromatography

The concentration of contaminants in the aqueous solution was determined by Headspace Gas Chromatography coupled to Mass Spectrometry (HS-GC-MS).

The analysis was carried out using an Agilent GC-MS system (Santa Clara, CA, USA) consisting of a GC 6850 Series II Network coupled to a Pal G6500-CTC injector and a Mass Selective Detector 5973 Network.

HS autosampler injector conditions are: incubation oven temperature 80 °C, incubation time 50 min, headspace syringe temperature 85 °C, agitation speed 250 rpm, agitation on time 30 s, agitation off time 5 s, injection volume 500 μL, fill speed 30 μL s^{-1}, syringe pull-up delay 5 s, injection speed 250 μL s^{-1}, pre-injection delay 0 s, post injection delay 2 s, syringe flush 30 s with nitrogen. The injected solutions consist of 100 μL of sample solutions, diluted in 10 mL of a aqueous solution saturated with NaCl, containing 10 μL of 500 mg L^{-1} of fluorobenzene in methanol as internal standard.

A DB-624 UI GC column (L = 20 m, I.D. = 0.18 mm, df = 1.00 μm film thickness, Agilent, Santa Clara, CA, USA) was used. High purity helium was the carrier gas with a constant flow rate of 0.7 mL min^{-1}. The oven temperature gradient started at 40 °C for 4 minutes and then ramped to 130 °C at 15 °C min^{-1}. The injector temperature was kept at 150 °C. All samples were injected in split mode (10 : 1).

The mass spectrometer operated in electron impact mode (positive ion, 70 eV). The source temperature and the quadrupole temperature were set to 230 °C and 150 °C respectively.

The mass spectra were acquired in full scan mode. The electronic scan speed was 1562 amu s^{-1} in a mass range from 30 to 300 amu. For identification and quantification of the target analyte the SIM (selected ion monitoring) chromatograms were extracted from the acquired signal by selecting the most abundant characteristic fragments at m/z = 62.49 (DCE), m/z = 73.57 (MTBE) and m/z = 91.92 (TOL). Chromatographic peak of analytes was identified by comparison of the retention time and the mass spectrum with standard compound and library data; quantitative analysis was performed using calibration curves.

Adsorption isotherms

Adsorption isotherms were determined using the batch method. Batch experiments were carried out in duplicate in 20 mL crimp top reaction glass flasks sealed with PTFE septa (Supelco, PA, USA). The flasks were filled in order to have the minimum headspace. A solid/solution ratio of 1 : 4 (mg mL^{-1}) was employed. After equilibration for 24 hours at a temperature of 25.3 ± 0.5 °C under stirring, the solids were separated from the aqueous solution using centrifugation (14 000 rpm for 30 min). To determine adsorbed quantities (q) and equilibrium concentrations (C_e), concentrations of TOL, MTBE and DCE were determined in solutions before and after equilibration with the zeolite. The uptake (q) was calculated as follows:

$$q = \frac{(C_0 - C_e)V}{m} \quad (1)$$

where C_0 is the initial concentrations in solution (mg L^{-1}); V is the solution volume (L); and m is the mass of sorbent (g). All experiments were carried out in duplicates (deviations were within 5%). Experimental isotherm data were fitted to two different models of competitive sorption isotherms (see eqn (2) and (3)). All the model parameters were evaluated by non-linear regression using MATLAB® software. The optimization procedure requires an error function to evaluate the goodness of fit of the equation to experimental data. Apart from the coefficient of determination (R^2), the sum of the residual square errors (SSE) was also used to measure the goodness-of-fit.

Thermal analyses

Thermogravimetric (TG) and differential thermal analysis (DTA) of zeolite samples after mixture adsorption was performed in air using an STA 409 PC LUXX®-Netzch operating at 10 °C min^{-1} heating rate, from room temperature (RT) to 900 °C.

X-ray powder diffraction (XRPD) data collection and refinement strategy

X-ray diffraction experiments were carried out at the high-resolution powder diffraction beamline ID22 at the European Synchrotron Radiation Facility, ESRF (Grenoble, France). Once diffracted, the incident X-ray (λ = 0.400031 Å) was directed through nine Si 111 analyser crystals and then collected in parallel by means of nine detectors. A subsequent data-reduction was performed to produce the equivalent step scan. X-ray diffraction patterns were recorded in the 0.5–19.5 2θ range. An automatic indexing of peaks, performed by means of the High Score Plus v.3.0 software, revealed the presence in DCE-MTBE and TOL-MTBE loaded-ZSM-5 patterns of peak doublets (*i.e.* 131/13-1, 311/31-1, 133/13-3, and 313/31-3) indicating the monoclinic $P2_1/n$ symmetry.

We investigated the changes of the crystal structure accompanying the mixture adsorption by performing Rietveld refinements using the EXPGUI interface, for General Structure Analysis System (GSAS) (2001).[29] Initial fractional atomic coordinates for the framework constituents in space group $P2_1/n$ were based upon the model determined by Pasti *et al.*[18] for as-synthesized ZSM-5. The peak profiles were modelled by a convolution of a double-exponential and a switch function with a pseudo-Voigt function; given the large number of structural parameters, the refinement was started by imposing severe constraints on the T–O bond distances. The weights of constraints were progressively released at convergence. Furthermore, the displacement parameters for a given atom type (*i.e.*, Si and O sites) were constrained to be equal, thus limiting the number of refined atomic displacement parameters to two. The instrumental background was modelled by a Chebyshev polynomial with 16 coefficients to refine. Table 1 lists the details of the data collection and Rietveld refinements. The refined atomic coordinates and isotropic thermal parameters of ZSM-5-loaded structures are given as ESI (Tables 2–5SI†).

Table 1 List details of the data collection and unit cell parameters of ZSM-5 unload and loaded with single DCE, TOL, MTBE molecules and binary mixtures of them

	ZSM-5[a]	ZSM-5-DCE[b]	ZSM-5-TOL[c]	ZSM-5-MTBE	ZSM-5-DCE-MTBE	ZSM-5-TOL-MTBE

Space group	$P2_1/n$	$P2_1/n$	$P2_1/n$	$P2_1/n$	$P2_1/n$	$P2_1/n$
a (Å)	19.900(1)	19.905(1)	19.907(1)	19.898(1)	19.900(1)	19.895(1)
b (Å)	20.117(1)	20.120(2)	20.118(1)	20.119(1)	20.116(1)	20.114(1)
c (Å)	13.389(1)	13.391(1)	13.393(1)	13.384(1)	13.387(1)	13.383(1)
β (°)	90.55(1)	90.58(1)	90.54(1)	90.57(1)	90.6(1)	90.59(1)
V (Å^3)	5359.9(3)	5362.7(1)	5363.0(1)	5358.1(1)	5358.6(1)	5355.2(1)
Wavelength (Å)	1.5417(1)	0.400031(1)	0.400031(1)	0.400031(1)	0.400031(1)	0.400031(1)
Refined pattern 2θ range (°)	3–110	0.7–25	1–24.56	1–24	1–24	1–24
R_{wp} (%)	9.12	9.2	19.8	16.7	12.4	15.4
R_p (%)	8.4	8.5	14.54	13.12	9.2	11.04
R_f^2 (%)	9.1	7.50	8.7	11.1	8.8	9
No. of contributing reflections	14 142	12 252	12 055	11 774	11 760	11 783
N_{obs}	5601	7239	7065	6357	6357	6477
N_{var}	289	282	276	364	356	359

[a] Pasti *et al.* 2012 (ref. 18). [b] Martucci *et al.* 2015 (ref. 2). [c] Rodeghero *et al.* 2015 (ref. 21). [d] In this work.

Results and discussion

Characterization of MTBE-DCE and TOL-MTBE loaded ZSM-5 by X-ray diffraction

X-ray diffraction studies were used to elucidate the detailed mechanism of DCE-MTBE-water and TOL-MTBE-water adsorption on the zeolite. After DCE-MTBE and TOL-MTBE mixture adsorption, the ZSM-5 diffraction peak positions were found to be similar (see ESI Fig. S1†). Consequently, one may conclude that unit-cell parameters were not remarkably modified (Table 1) after adsorption. In the low 2θ region highlighted in Fig. S1,† peak intensities (that are strongly dependent on the arrangement and occupancy of species in zeolite cavities) are different in the two patterns suggesting that guest molecules enter ZSM-5 channels. Iterating the Rietveld cycles for ZSM-5 loaded with DCE-MTBE and TOL-MTBE mixtures, using the silica framework model without any inclusion of adsorbed guest molecules, the following residual values for fitting profiles with respect their correspondent diffraction patterns were obtained: R_{wp} 23.96 and R_p 18.35 for ZSM-5-MTBE-DCE and R_{wp} = 23.45 and R_p = 19.57 for ZSM-5-TOL-MTBE. Therefore, difference Fourier maps calculated at this stage revealed the presence of groups of electron density peaks corresponding to adsorption of organics, which had not yet been modelled. Considering the geometry of the DCE, TOL and MTBE molecules, the maps suggested the presence of more than the one molecular species with different orientations in the channel systems. Incorporating this model for the guest species into further Rietveld refinement cycles, the residual values in the Rietveld fit have been drastically decreased to R_{wp} = 9.24 and R_p = 7.61 for ZSM-5-DCE-MTBE and R_{wp} = 9.10 and R_p = 8.25 for ZSM-5-TOL-MTBE, respectively. The refined unit cell parameters for the ZSM-5-TOL-MTBE system are: a (Å) = 19.895(1); b (Å) = 20.114(1); c (Å) = 13.383(1); β angle = 90.59(1) and, finally, the refined unit cell volume V (Å^3) was 5355.2(1). In the case of ZSM-5-DCE-MTBE mixture the unit cell parameters are the following: a (Å) = 19.900(1); b (Å) = 20.116(1); c (Å) = 13.387(1); β angle = 90.6(1) and the unit cell volume V (Å^3) was 5358.6(1).

ZSM-5 loaded with single component: DCE, TOL and MTBE

As far as it concerns ZSM-5-DCE system, Rietveld refinement indicated two crystallographic independent DCE sites namely DCE1 (located near SC-channels) and DCE2 (lied in the ZZ 10-ring channel), respectively (see Fig. 1a and b). As reported by Martucci *et al.*,[2] the refined occupancies seem to indicate that DCE molecules prefer to be hosted in the DCE1 site more than in the DCE2 one (84% occupancy in DCE1 *vs.* 74% in DCE2). On the whole, the total amount of DCE adsorbed was about 6.5 DCE/u.c. (corresponding to about 11.5% in zeolite dry weight, dw). Similarly, after TOL adsorption 30, the difference Fourier map indicated TOL molecules to distribute over two crystallographic independent sites (TOL1

and TOL2, respectively, Fig. 1a and b. TOL1 site (occupied in 85% of cases), was close to SC-channels, while TOL2, (occupied in 65% of cases) was located at the intersection between SC and ZZ channels (Fig. 1a and b). On the basis of refined occupancies, 6 toluene molecules (corresponding to about 8.55% w/w in zeolite dry weight) were detected.

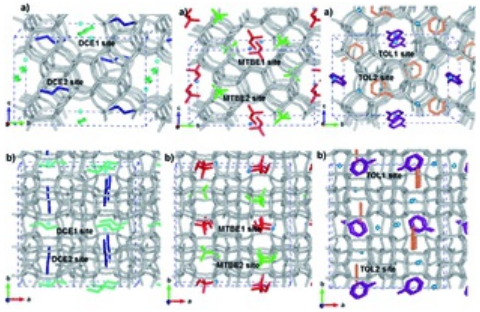

Fig. 1 Unit cells with the modelled atoms of MTBE, DCE, and TOL adsorbed molecules and the location sites (SC straight channel – ZZ sinusoidal channel) along *a* and *c* directions, respectively.

The structure refinement of ZSM-5 after MTBE adsorption was carried out in this work, by using the same unloaded ZSM-5 (CBV28014, Zeolyst) as well as the same experimental conditions reported elsewhere.[2,30] Our refinement allowed us to recognize two crystallographic independent extraframework sites. The first one, MTBE1 is located approximately close to the SC channel (Fig. 1a and b); the second one, MTBE2 (Fig. 1a and b) is positioned in the ZZ channel. On the whole, 8 MTBE molecules (corresponding to roughly 11% w/w zeolite dry weight) were detected. In all systems, additionally extra-framework sites were detected and attributed to water molecules (about 1.5% w/w). According to ref. 2, 6, 22, 27 and 31, the distances refined with the Rietveld method suggested the occurrence of MTBE-, DCE-, TOL-water oligomers (clusters or short chains) strongly interacting with the framework oxygens.

To summarize, occupation values have allowed to obtain, from the pure component Rietveld refinements, the preferential adsorption sites of DCE, TOL and MTBE molecules in the structures. The most populated sites (MTBE1, DCE1 and TOL1) are located near the SC channel thus representing a significantly stable sorption site for these organics. Additional guest molecules are adsorbed in the ZZ channels or at the intersection between SC and ZZ channels (MTBE2, DCE2 and TOL2 sites, respectively). Based on TOL,[30] DCE[2] and MTBE fractional coordinates (this work), competition for adsorption can be expected if these molecules are simultaneously present in the system. To further support this idea and to improve our understanding of the behaviour of molecules inside the structure, all the intermolecular distances between DCE, TOL and MTBE were calculated. The short interdistance values (MTBE1-DCE2 0.43 (1), MTBE2-DCE1 0.57 (1), MTBE1-TOL2 0.69 (1), MTBE2-DCE1 1.10 (1), TOL1-DCE1 0.58 (1), TOL2-DCE2 0.50 (1)), are clearly incompatible with a simultaneous occupancy by more than one molecule, thus strengthening the need of competitive studies.

ZSM-5 loaded with TOL-MTBE and DCE-MTBE binary mixtures

Rietveld structure refinements provided information about the relative position of molecules inside the structure after TOL-MTBE and DCE-MTBE mixture adsorption. In ZSM-5-TOL-MTBE, TOL molecules are confined only in the TOL1 site (about 3.8 molecules, corresponding to approx. 5.3% in zeolite dw), near the SC channel. TOL2 site (located in the channels intersections or ZZ) is now empty (Fig. 2a and b). MTBE molecules are confined in MTBE2 site (ZZ channel) (roughly 3.4 MTBE molecules per unit cell, corresponding to approx. 4.5% in zeolite dw). TG data confirmed this level of incorporation of organics. The total weight loss at 900 °C is approximatively 13% w/w, in very good agreement with the refined occupancies, as well as the adsorption data (*vide infra*).

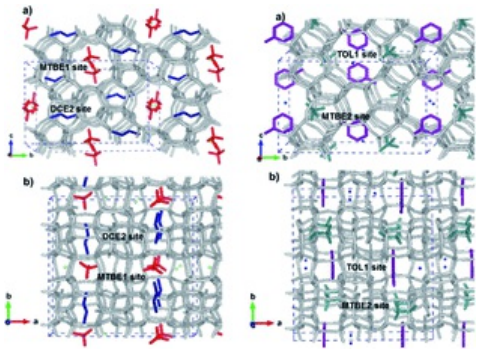

Fig. 2 Unit cells with the modelled atoms of ZSM-5-DCE-MTBE-, and ZSM-5-TOL-MTBE adsorbed molecules and the location sites (SC straight channel – ZZ sinusoidal channel) along *a* and *c* directions, respectively.

As shown in Fig. 2SI,† the TG curve shows a first weight loss below 100 °C, which can be ascribed to the elimination of species weakly bonded to the surface (~3% w/w). Above this temperature, the slope suddenly changes most likely following the decomposition/release of extraframework species (MTBE, TOL and water molecules) embedded within the MFI pores (weight loss roughly 10.0% dw/w). A similar trend was also observed for ZSM-5-DCE-MTBE (Fig. 2SI†).

As far as it concerns the relative position of MTBE and DCE molecules inside the structure, two independent extraframework sites are again localised. MTBE (3.3 molecules p.u.c. corresponding to 4.5% in zeolite dw) is confined near the SC channel (MTBE1 site in Fig. 2a and b), whereas DCE (2.7 molecules p.u.c. corresponding to 4.2% in zeolite dw) is in the ZZ channel (DCE2 site). Difference Fourier maps calculated for both ZSM-5-DCE-MTBE and ZSM-5-TOL-MTBE revealed the occurrence of a low amount of co-adsorbed water in both the systems (about 4.0 molecule p.u.c. corresponding to approx. 1% w/w in zeolite). The refined distances between the framework oxygen, water oxygen atoms and organic molecules suggested the occurrence of water-MTBE and water-MTBE-DCE complexes interacting with the framework. The presence of organic–water complexes (clusters or short chains) stabilizing the guest structure within the zeolite host framework[6] has also been recently observed in high-silica mordenite,[5,31,32] as well as in Y zeolite after DCE[22] and MTBE adsorption from aqueous solutions.[21] This finding could possibly explain the higher MTBE adsorption capacity (11% found in ref. 20 and reconfirmed in ref. 21, with respect to that observed from gas phase systems.[26] After loading, the changes in the framework geometry can be monitored by following both the ellipticity (ε) and Crystallographic Free Area (C.F.A.) of the 10-ring channels.[33] Table 2 reports the dimensions of both sinusoidal and straight channels, assuming a spherical shape with radius of 1.35 Å (ref. 34) for the framework oxygen atoms. The resulting apertures appear larger than those reported for the unloaded ZSM-5 but smaller than the maximum value diameter 7.6 Å) for an ideal circular 10-ring channel (C.F.A. = 24.5 Å^2). The overall effect of these variations accounts for the slight cell volume contraction observed with respect to the as-synthesized material.

Table 2 The ellipticity (ε = largest/shortest oxygen–oxygen distances) and C.F.A. (assuming an oxygen ionic radius of 1.35 Å) of the apertures of unloaded ZSM-5, as well as after DCE, MTBE, TOL, DCE-MTBE and TOL-MTBE adsorption

Straight channel (SC-A)	ε	CFA	Straight channel (SC-B)	ε	CFA
ZSM-5 (*)	1.03	22.68	ZSM-5 (*)	1.02	22.68
ZSM-5-DCE (**)	1.08	24.14	ZSM-5-DCE (**)	1.08	23.51
ZSM-5-TOL (***)	1.03	24.4	ZSM-5-TOL (***)	1.04	23.61
ZSM-5-MTBE	1.09	24	ZSM-5-MTBE	1.06	23.67
ZSM-5-DCE-MTBE	1.07	24.16	ZSM-5-DCE-MTBE	1.04	23.67
ZSM-5-TOL-MTBE	1.09	24.06	ZSM-5-TOL-MTBE	1.05	23.59
Sinusoidal channel (ZZ-A)	**ε**	**CFA**	**Sinusoidal channel (ZZ-B)**	**ε**	**CFA**
ZSM-5 (*)	1.04	21.65	ZSM-5 (*)	1.06	22.65
ZSM-5-DCE (**)	1.09	24.37	ZSM-5-DCE (**)	1.12	23.12
ZSM-5-TOL (***)	1.12	23.63	ZSM-5-TOL (***)	1.06	23.68
ZSM-5-MTBE	1.07	24.3	ZSM-5-MTBE	1.1	22.91
ZSM-5-DCE-MTBE	1.05	24.28	ZSM-5-DCE-MTBE	1.1	23.15
ZSM-5-TOL-MTBE	1.06	24.35	ZSM-5-TOL-MTBE	1.1	22.95

Adsorption from binary mixtures

Isotherm profiles from experiments with DCE alone and with a DCE/MTBE mixtures are shown in Fig. 3a. For competitive experiments, the isotherm of DCE in presence of MTBE is below its isotherm in the single component system (see Fig. 3a), in at least a portion of the adsorption curve, indicating that MTBE and DCE compete for the adsorption onto ZSM-5 within the concentration range shown. Isotherms of DCE alone and DCE in presence of MTBE mainly diverge at the highest concentration range thus suggesting that the extent of competition can change with concentration. A similar trend was also observed for the adsorption of TOL and of TOL/MTBE mixtures (see Fig. 3b), thus confirming the competitive nature of the adsorption of VOCs mixtures on zeolites.

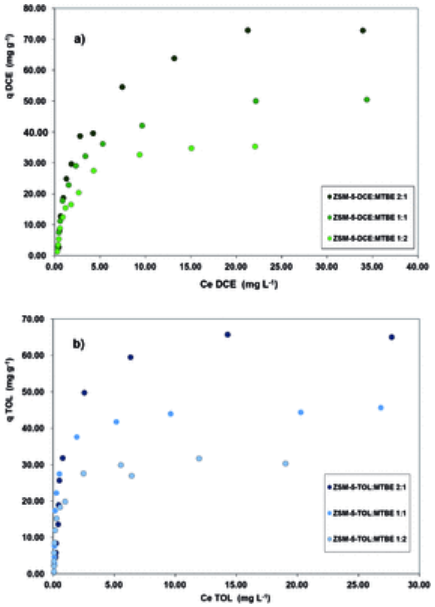

Fig. 3 Experimental uptake data of (a) DCE-MTBE and (b) TOL-MTBE aqueous mixtures in ZSM-5.

Many models have been proposed to describe competitive adsorption from liquid media[35,36] and, as mentioned in ref. 37, the selection of an isotherm model is usually based on literature data or intuition, or it uses the method of trials and errors. In such cases, a model that well fits the experimental data would not adequately describe the actual physical behaviour of the adsorption system. The isotherm selected could lead to significant bias when employed in selected concentration ranges. Therefore, the choice of a model which not only accounts well for the experimental data in the considered cases but also has a physical meaning, is preferable. The physical description of the adsorption systems derive from the structural refining investigation above reported.

All of the three compounds are located into two different sites of the ZSM-5, these two sites cannot be simultaneously occupied by two different compounds and each site is available for a single molecule (monolayer).

On the basis of this information, the competitive bi-Langmuir model (CBLM)[37] seems to be suitable for describing the adsorption of these mixtures. For each of the two compounds (i = 1, 2), the CBLM is given by:

$$q_{e,i} = \frac{q_{s,a,i} K_{a,i} C_{e,i}}{1 + K_{a,1} C_{e,1} + K_{a,2} C_{e,2}} + \frac{q_{s,b,i} K_{b,i} C_{e,i}}{1 + K_{b,1} C_{e,1} + K_{b,2} C_{e,2}}, \quad (i = 1, 2) \qquad (2)$$

where q_e (mg g^{-1}) is the amount of adsorbate per unit mass of adsorbent at the equilibrium with a solution of concentration C_e (mg L^{-1}), q_s (mg g^{-1}) the saturation capacity and K (L mg^{-1}) the equilibrium constant for the adsorption, the subscripts refer to sites a and b, and to compounds 1 and 2 of the binary mixture, respectively. However, the adsorption of these three compounds on this same zeolite was recently studied,[21,22,30] and a Langmuir model was found satisfactory to fit the unary solutions of all of the three compounds. Based on the information afforded by single-component isotherms, the classical competitive Langmuir model (CLM) isotherm (i = 1, 2), is given by:

$$q_{e,i} = \frac{q_{s,i} K_i C_{e,i}}{1 + \sum K_i C_{e,i}} \qquad (3)$$

The CLM can, in fact, be applied to mixtures of components obeying Langmuir behaviour in single-solute system, and when the saturation capacities of the components are similar to each other. To account for differences in site availability for the components of the mixture, a modified model can be applied. In this latter model a number of sites with non-competitive adsorption was added and these additional sites are proportional to the difference between the maximum loadings of the two species.[37] The confidence limits, calculated at 95% of probability, of the saturation capacities obtained from the single component adsorption isotherms were 88–100 mg g^{-1}, 77–87 mg g^{-1} and 113–127 mg g^{-1} for MTBE, TOL and DCE respectively. These values correspond to 6.4–7.3, 5.4–6.1 and 7.3–8.3 molecules per unit cell. The differences in saturation capacities (molecules per unit cell) for both TOL-MTBE and MTBE-DCE mixtures were in the order of

10%, which can be considered acceptable for the applicability of CLM.[38] Both CLM and CBLM have been used to fit experimental adsorption data of organic species on microporous materials.[39] Another model often employed to describe adsorption from binary mixtures[15] is the ideal adsorbed solution theory (IAST). However, it has been shown that IAST does not provide reliable results for the adsorption of alcohols from aqueous solution onto hydrophobic zeolites[16,40] probably due to strong solute–solvent interactions (hydrogen bonds). Deviations in IAST model can also be due to framework deformation upon adsorption,[41–43] therefore, IAST seems to be not adequate to fit the data of the present work since the adsorption of the three selected compounds occurs with a slight cell volume modification as above mentioned.

The adsorption of both the components of the aqueous binary mixtures on zeolite ZSM-5 at different concentrations have been determined. The effect of MTBE on the competitive adsorption of TOL and DCE is also shown in Fig. 4a, that reports the adsorption selectivity (α) calculated as:

$$\alpha_{\mathrm{TOL/MTBE}} = \frac{x_{\mathrm{z,TOL}} / x_{\mathrm{a,TOL}}}{x_{\mathrm{z,TMTBE}} / x_{\mathrm{a,MTBE}}} \qquad (4)$$

where $x_{\mathrm{z,TOL}}$ and $x_{\mathrm{z,MTBE}}$ are the adsorbed quantity per unit mass of adsorbent material, of TOL and MTBE onto ZSM-5 and $x_{\mathrm{a,TOL}}$ and $x_{\mathrm{a,MTBE}}$ are the concentration of TOL and MTBE in aqueous solution, respectively. Analogously, a similar relation can be obtained for the DCE/MTBE adsorption system (see Fig. 4b). The ZSM-5 selectivity towards TOL with respect to MTBE decreases with increasing MTBE concentration. Operation conditions in the lower concentration are selective to TOL which has a higher adsorption strength as determined in unary adsorption isotherm. On the contrary, the selectivity of ZSM-5 for DCE slightly increases with increasing MTBE concentration, thus confirming that the saturation capacities and adsorption constants of these compound are similar (see Fig. 4).

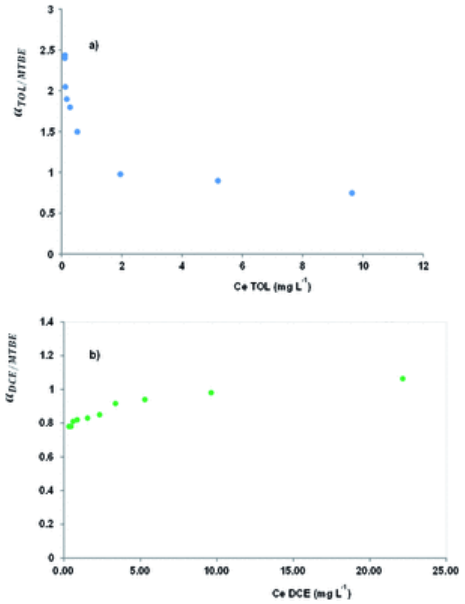

Fig. 4 ZSM-5 selectivity plot (a) TOL-MTBE system at equimolar condition (1 : 1) (b) DCE-MTBE system at equimolar condition (1 : 1).

Three dimensional plot of the adsorbed amount of MTBE and DCE on the ZSM-5 zeolite from binary mixtures of TOL-MTBE and DCE-MTBE, are shown in Fig. 5.

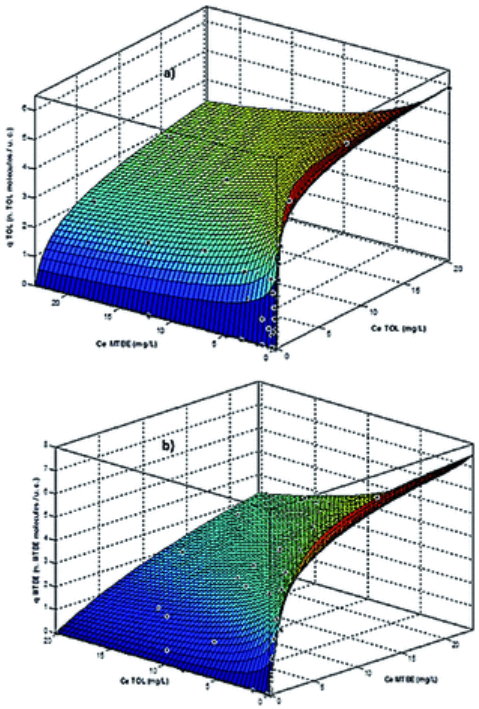

Fig. 5 Surface fitting (a) number of TOL adsorbed molecules per ZSM-5 unit cell *vs.* the equilibrium concentrations of TOL and MTBE in aqueous solution, (b) number of MTBE adsorbed molecules per ZSM-5 unit cell *vs.* the equilibrium concentrations of TOL and MTBE in aqueous solution. The points represent the experimental data.

The contour surfaces are the competitive dual site Langmuir isotherms generated by non-linear fitting procedure. The results of estimated parameters for the CBLM and CLM are reported in Table 3.

Table 3 Isotherm parameters for the adsorption of TOL-MTBE and DCE-MTBE on ZSM-5 (@25 °C)

				R^2	SSE
ZSM-5-TOL-MTBE	TOL	*Langmuir*			
		q_S	83.7	0.9476	1559.8
		b	2.418		
		Bilangmuir			
		$q_{S,A}$	48.2	0.9879	680.6
		b_1	0.683		
		$q_{S,B}$	37.1		
		b_2	0.234		
	MTBE	*Langmuir*			
		q_S	97.7	0.9374	1710.5
		b	0.408		

		Bilangmuir			
		$q_{s,1}$	62	0.9821	728.3
		b_1	0.731		
		$q_{s,2}$	38		
		b_2	0.314		
ZSM-5-DCE-MTBE	DCE	*Langmuir*			
		q_s	108	0.9146	2052.8
		b	0.219		
		Bilangmuir			
		$q_{s,1}$	64	0.9759	908.7
		b_1	0.283		
		$q_{s,2}$	48		
		b_2	0.144		
	MTBE	*Langmuir*			
		q_s	96.8	0.8926	2870
		b	0.427		
		Bilangmuir			
		$q_{s,1}$	62	0.9721	912.3
		b_1	0.661		
		$q_{s,2}$	34		
		b_2	0.247		

It can be seen that for binary mixtures, the determination coefficients of CBLM gave a better fit than CLM. *F* test was applied to the standard deviation of the residuals to examine if the difference of the two models was statistically significant, taking into account the different number of parameters in the fitting equations.

Conclusions

In this work an exhaustive picture of VOCs binary mixture adsorption on microporous MFI material by combining microscopic (*i.e.* adsorption isotherms) and macroscopic (*i.e.* structural refinements) information is provided. Three representative water contaminants (toluene, methyl *tert*-butyl ether and 1,2-dichloroethane) were selected as test molecules. Our results highlighted that with respect to the single-component data, the loading of all of the three compounds was reduced in the presence of a second component in the mixture. The adsorption data of dual component mixtures were fitted with a Langmuir model which was chosen on the basis of the results obtained from X-ray diffraction studies of the adsorbent material loaded with equimolar binary mixtures.

The Rietveld structural investigation provided informations about the relative position of molecules inside the structure after TOL-MTBE and DCE-MTBE mixture adsorption. The short refined intermolecular distances between the adsorption sites of MTBE, DCE and TOL inside the zeolite framework clearly prevented the simultaneous occupancy of one site by more than one component, when these compounds are adsorbed from binary mixtures. This original approach of integrating structural information to thermodynamic equilibrium data allowed us to obtain an excellent model system for realistically describing the adsorption process and helping in the interpretation of the adsorption mechanisms. To the best of our knowledge this is one of first works showing the correlation between microscopic XRD molecular information and macroscopic adsorption experimental data for binary mixtures.

Finally, the different properties of the selected VOCs, adsorption studies of these species also provide insights into zeolite selectivity for VOC removal process. Consequently, these findings are of certain interest for scientists working with zeolite-based technologies to treat natural and wastewaters where a mixture of contaminants often occur.

Acknowledgements

The authors thank the Italian University and Scientific Research Ministry (Grant PRIN 2012ATMNJ 003) and the Laboratory Terra&Acqua Tech, Technopole of Ferrara of Emilia-Romagna High Technology Network. Dr Valentina Costa from the University of Ferrara is acknowledged for technical support.

Notes and references

1 *Handbook of Zeolite Science and Technology*, ed. S. M. Auerbach, K. Carrado and P. Dutta, Marcel Dekker, New York, 2004.

2 A. Martucci, E. Rodeghero, L. Pasti, V. Bosi and G. Cruciani, *Microporous Mesoporous Mater.,* 2015, **215,** 175.

3 R. Barrer, *Zeolites and clay minerals as sorbents and molecular sieves*, Academic Press, London, 1978.

4 R. H. Jensen, *Refining processes: setting the scene. In Zeolites for Cleaner Technologies,* ; ed. M. Guisnet and J.-P. Gilson, Imperial College Press: London, 2002, ; **vol. 3.**

5 A. Martucci, L. Pasti, M. Nassi, A. Alberti, R. Arletti, R. Bagatin, R. Vignola and R. Sticca, *Microporous Mesoporous Mater.,* 2012, **151,** 358.

6 E. Güvenç and M. G. Ahunbay, *J. Phys. Chem. C,* 2012, **116** (41), 21836.

7 S. Li, V. A. Tuan, R. D. Noble and J. L. Falconer, *Environ. Sci. Technol.,* 2003, **37** (17), 4007.

8 A. Martucci, I. Braschi, L. Marchese and S. Quartieri, *Mineral. Mag.,* 2014, **78** (5), 1115.

9 C. Perego, R. Bagatin, M. Tagliabue and R. Vignola, *Microporous Mesoporous Mater.,* 2013, **166** (15), 37.

10 R. Vignola, R. Bagatin, A. De Folly D'Auris, C. Flego, M. Nalli, D. Ghisletti, R. Millini and R. Sisto, *Chem. Eng. J.,* 2011, **178** (15), 204.

11 R. Vignola, R. Bagatin, A. De Folly, D. Massara, E. P. D. Ghisletti, R. Millini and R. Sisto, *Chem. Eng. J.,* 2011, **178** (15), 210.

12 I. Braschi, S. Blasioli, E. Buscaroli, D. Montecchio and A. Martucci, *J. Environ. Sci.,* 2016, **48,** 302.

13 G. Bellussi, R. Millini, P. Pollesel and C. Perego, *New J. Chem.,* 2016, **40,** 4061.

14 A. W. Thornton, D. A. Winkler, M. S. Liu, M. Haranczyk and D. F. Kennedy, *RSC Adv.,* 2015, **5,** 44361.

15 R. Krishna, *Phys. Chem. Chem. Phys.,* 2015, **17,** 39.

16 R. Krishna and J. M. van Baten, *Langmuir,* 2010, **26,** 8450.

17 J. Pires, A. Carvalho and M. B. de Carvalho, *Microporous Mesoporous Mater.,* 2001, **43** (3), 277.

18 S. Brosillon, M.-H. Manero and J. N. Foussard, *Environ. Sci. Technol.,* 2001, **35** (17), 3571.

19 P. Monneyron, M. H. Manero and J. N. Foussard, *Environ. Sci. Technol.,* 2003, **37** (11), 2410.

20 A. Erdem-Senatalar, J. A. Bergendahl, A. Giaya and R. W. Thompson, *Environ. Eng. Sci.,* 2004, **21** (6), 722.

21 A. Martucci, I. Braschi, C. Bisio, E. Sarti, E. Rodeghero, R. Bagatin and L. Pasti, *RSC Adv.,* 2015, **5** (106), 86997.

22 L. Pasti, A. Martucci, M. Nassi, A. Cavazzini, A. Alberti and R. Bagatin, *Microporous Mesoporous Mater.,* 2012, **160,** 182.

23 A. Martucci, L. Pasti, M. Nassi, A. Alberti, R. Arletti, R. Bagatin, R. Vignola and R. Sticca, *Microporous Mesoporous Mater.,* 2012, **151,** 358.

24 R. Krishna and J. M. van Baten, *Langmuir,* 2010, **26** (13), 10854–10867.

25 R. Krishna and J. M. van Baten, *J. Phys. Chem. C,* 2010, **114** (30), 13154–13156.

26 M. G. Ahunbay, O. Karvan and A. Erdem-Şenatalar, *Microporous Mesoporous Mater.,* 2008, **115** (1), 93.

27 R. Arletti, A. Martucci, A. Alberti, L. Pasti, M. Nassi and R. Bagatin, *J. Solid State Chem.,* 2012, **194,** 135.

28 S. Li, V. A. Tuan, R. D. Noble and J. L. Falconer, *Environ. Sci. Technol.,* 2003, **37** (17), 4007.

29 A. C. Larson and and R. B. Von Dreele, *"General Structure Analysis System (GSAS)", Los Alamos National Laboratory Report LAUR*, 2000, p. 86

30 E. Rodeghero, A. Martucci, G. Cruciani, R. Bagatin, E. Sarti, V. Bosi and L. Pasti, *Catal. Today,* 2016, 10.1016/j.cattod.2015.11.031, in press

31 R. Arletti, A. Martucci, A. Alberti, L. Pasti, M. Nassi and R. Bagatin, *J. Solid State Chem.,* 2012, **194,** 135.

32 A. Martucci, L. Leardini, M. Nassi, E. Sarti, R. Bagatin and L. Pasti, *Mineral. Mag.,* 2014, **78** (5), 1161.

33 C. Baerlocher, W. Meier and and D. Olson, *Atlas of zeolite framework types,* ; Elsevier: Amsterdam, 2001.

34 R. D. Shannon, *Acta Crystallogr.,* 1976, **A32,** 751.

35 T. Longlong, Z. Xin, Q. Wei, L. Dan, J. Qiang, L. Jin, Y. Yuanlv, L. Zhan and W. Wangsuo, *RSC Adv.,* 2014, **4,** 58536.

36 J. Zhu, A. M. Katti and G. Guiochon, *J. Chromatogr. A,* 1991, **552,** 71.

37 I. Quiñones and G. Guiochon, *J. Chromatogr. A,* 1996, **734** (1), 83.

38 J. S. Jain and and V. L. Snoeyink, *Adsorption from bisolute systems on active carbon. Journal (Water Pollution Control Federation)*, 1973, p. 2463

39 G. Guiochon, A. Felinger and and D. G. Shirazi, *Fundamentals of preparative and nonlinear chromatography*, Academic Press, San Diego, 2nd edn, 2006.

40 T. C. Bowen and L. M. Vane, *Langmuir,* 2006, **22** (8), 3721.

41 P. Bai, M. Tsapatsis and J. I. Siepmann, *Langmuir,* 2012, **28** (44), 15566.

42 C. M. Simon, B. Smit and M. Haranczyk, *Comput. Phys. Commun.,* 2016, **200,** 364.

43 Z. Li and S. Singh, *J. Phys. Chem. A,* 2008, **112** (37), 8593.

Queries and Answers

Query: For your information: You can cite this article before you receive notification of the page numbers by using the following format: (authors), RSC Adv., (year), DOI: 10.1039/c6ra08872d.

Answer: OK

Query: Please carefully check the spelling of all author names. This is important for the correct indexing and future citation of your article. No late corrections can be made.

Answer: All names are correct. Luisa Pasti, Elisa Rodeghero, Elena Sarti, Valentina Bosi, Alberto Cavazzini, Roberto Bagatin, Annalisa Martucci

Query: Do you wish to indicate the corresponding author(s)? If so, please specify the corresponding author(s).

Answer: Correspondin authors: Annalisa Martucci Luisa Pasti

Query: Do you wish to add an e-mail address for the corresponding author? If so, please supply the e-mail address.

Answer: mrs@unife.it; psu@unife.it

Query: Please check that the inserted Graphical Abstract text is suitable. Please ensure that the text is no longer than 250 characters (including spaces).

Answer: Ok

Query: “Pasti” is not cited as an author of ref. 18. Please indicate any changes that are required here.

Answer: The correct reference number is 22.

Query: Text has been provided for footnote d in Table 1, but there does not appear to be a corresponding citation in the table. Please indicate a suitable location for the footnote citation.

Answer: in column n.4, the text must be modified as follows: ZSM-5-MTBE footnote d

Query: Please explain the significance of the asterisk symbol used in the “Table 2” If this is intended to be a link to a footnote then please provide the appropriate text.

Answer: ***(*)Pasti et al. 2012 [22], (**) Martucci et al. 2015 [2], (***) Rodeghero et al. 2015 [30], (****) in this work.***

Query: Fig. 5 appears to be of low resolution and therefore appears rather blurred. Would you like to resupply the image at higher resolution (preferably as a TIF file at 600 dots per inch)?

Answer: see attachment

Query: Ref. 30: Can this reference be updated?

Answer: This reference is always in press